Research Article GU J Sci, Part A, 11(2): 264-273 (2024) 10.54287/gujsa.1435807

Gazi University
Journal of Science
PART A: ENGINEERING AND INNOVATION
http://dergipark.org.tr/gujsa

HR-XRD and AFM Analysis of AlN/SiC Structures for Optoelectronic Device Applications

Ozlem BAYAL[1*] Durmus DEMIR[1] Ahmet Kursat BILGILI[1] Naki KAYA[2] Mustafa Kemal OZTURK[1] Sukru KALAYCI[3]

[1] Gazi University, Photonics Research and Application Center, Ankara, Türkiye
[2] Kafkas University, Kağızman Vocational School, Optician Program, Türkiye
[3] Gazi University, Technical Sciences Vocational School, Ankara, Türkiye

Keywords
AlN
SiC
MOCVD
HR-XRD
UDM

Abstract
In this paper, we examined the successful growth of AlN on SiC substrate using molecular beam epitaxy technique (MBE). The AlN buffer layers are grown with (100, 130, 140 and 150 nm) thickness. XRD technique was used to analyze the four samples of Wurtsite structure including strain cases, dislocation densities and other micro-structural properties. XRD peak broadening data are used to determine crystallite size and strain values by using Williamson-Hall (WH) method. High resolution X-Ray Diffraction (HR-XRD) peak analysis method is used with Scherrer, WH, modified WH, uniform deformation model (U-DM), uniform stress deformation model (US-DM), uniform deformation energy density model (UDE-DM). Crystallite size, strain, stress, energy density values are determined by using young module. According to the results obtained from our data, it is observed that the energy value sharply decreases and then increases. This behavior of energy density is consistent with the strain and stress behaviors. It has been noticed that AlN buffer layers grown without tension and relaxation are more suitable for optoelectronic devices. Therefore, it is understood that the thickness values of AlN buffer layers are important.

Cite

Bayal, O., Demir, D., Bilgili, A. K., Kaya, N., Ozturk, M. K., & Kalayci, S. (2024). HR-XRD and AFM Analysis of AlN/SiC Structures for Optoelectronic Device Applications. *GU J Sci, Part A*, *11*(2), 264-273. doi:10.54287/gujsa.1435807

Author ID (ORCID Number)

0000-0003-0718-9734	Ozlem BAYAL
0000-0002-6470-6534	Durmus DEMIR
0000-0003-3420-4936	Ahmet Kursad BILGILI
0000-0003-2287-676X	Naki KAYA
0000-0002-8508-5714	Mustafa Kemal OZTURK
0000-0002-8643-6731	Sukru KALAYCI

Article Process

Submission Date	12.02.2024
Revision Date	18.03.2024
Accepted Date	03.04.2024
Published Date	27.05.2024

1. INTRODUCTION

Semiconductor group elements are used to form computer chips, cell phones, solar cells, light emitting diodes and similar modern devices. Recent technological improvements gave hand to investigate and develop new materials. At the same time many technological obstacles are met during these investigations and they need to be come over. Improvements in semiconductor industry are limited with applications of materials used during device production (Bilgili et al., 2021). Diamond, Silicon carbitte (SiC), Alliminium nitrite (AlN) and Gallium nitrite (GaN) are materials which have efficiency while operating at high temperature, power and frequency. Many of research on epitaxial film growth are made with II-VI and III-V group compounds such as GaAs and GaP until GaN is discovered by Shuji Nakamura (Nakamura, 1995; Akbas & Ozturk, 2023).

III group nitrites played an important role in development of blue laser technology. GaN based blue lasers are constructed by the help of GaN alloys. Although this is a big step in the field, there are many problems about production of high quality GaN alloys. Because of difficulties on production of mono-crystals with nitrite materials, growth of nitrite thin films on different substrates is needed (Akpinar et al., 2020). One of the

*Corresponding Author, e-mail: ozlembayal@gmail.com

problems is about %13 lattice mismatch between GaN and sapphire. This situation effects device performance in a bad way. SiC together with nitrites is used as an alternative to GaN because it has less lattice mismatch (Nakamura et al., 1994).

It is reported that LEDs grown on sapphire by using GaN alloy with MOCVD technique, has high light emitting efficiency (Nakamura, 1995). Performance of these devices is extremely high if dislocation density about 10^{10} cm^{-2} is taken into account (Lester et al, 1995). Defect density is high, because of great lattice mismatch between GaN and substrates. First LED with high luminesance is produced by (Nakamura et al., 1995). This success increased interest on GaN that can be used as blue light source.

Including lattice match and thermal expansion many similar properties of GaN and SiC give hand to produce devices with developed structural and optical properties (Sasaki & Matsuoka, 1988; Lin et al., 1993). Sasaki and Matsuoka (1988), grow GaN on SiC substrate by using MOCVD technique. They used high purity amonia as Nitrogen source. AlN is used as buffer layer between GaN and SiC because AlN resembles SiC in structural terms (Sasaki & Matsuoka, 1988). AlN is an important material that is used for improvement of optoelectronic devices and it has 6.2 eV band gap. Because of its high drift velocity, it is used for high power and high frequency applications. AlN is preferred for substrates without cracks among III nitrite semiconductors. So far there have been great development in the growth of bulk and layer AlN. In addition to this, device performance is limited on sapphire, Si and SiC substrates because of twist inducted by strain or cracks (Uehara et al., 2003; Yang, 2011) In this respect, stable strain analysis and to understand mechanical properties of AlN films is important. There are many ways to find out these properties. XRD is one of the sensitive and unharming method for these analysis (Rong et al., 2016).

In this study, structural properties of AlN alloy grown on SiC substrate by using MOCVD, are investigated. AlN/SiC structure, includes (100, 130, 140 and 150 nm) thick AlN buffer layers in four different samples. Generally, AlN buffer layer is used for maintaining lattice match in devices such as high electron mobility transistors (HEMTs) and LEDs. Decreasing of lattice mismatch gives hand to decreasing dislocations and producing high quality devices. XRD results showed that samples are in Wurtsite structure (Mote et al., 2012).

2. MATERIAL AND METHOD

All samples are grown with low pressure MOCVD technique on 4H-SiC substrate. Trimethylaliminium (TMAl) and NH3 are used as source for Al and N respectively. Hydrogen (H_2) is needed by using carrier gas. Before growth of AlN, SiC substrates are annealed at 1080°C to remove dirts on its surface. In all samples, 10 nm thick AlN is grown under low reactor pressure and at 845°C growth temperature. Later, reactor temperature is adjusted as (1105, 1025, 975 and 1055°C) for all samples 1, 2, 3 and 4 respectively. AlN main layer is grown under low reactor pressure for all samples respectively. During this growth NH3 flow rate is adjusted as 50, 1000, 1000 and 50 sccm. respectively. As the result of this growth operation, 100, 130, 140 and 150 nm thick AlN buffer layers are formed for samples 1, 2, 3 and 4. Growth conditions for samples are given in Table 1.

Table 1. *Growth conditions of samples 1, 2, 3 and 4*

Sample	Thickness (nm)	Growth ratio (um/h)	P (mbar)	T1 °C	T2 °C	TMAl flux (sccm)	NH3	AFM (roughness) (nm)
1	100	0.45	30	1105	1130	25	50	4.04
2	130	0.33	50	1025	1070	15	1000	3.71
3	140	0.33	50	975	1000	15	1000	3.63
4	150	0.45	30	1055	1080	25	50	3.22

3. RESULTS AND DISCUSSION

Crystallite size is calculated with equation (1). This equation comes from Scherer method.

$$\beta = \frac{k\lambda}{L\cos\theta} \tag{1}$$

Parameters in this method are gained from HR-XRD pattern using Scherrer method (Pandey et al., 2021). In equation (1) k is approximately equal to 1. Lambda is the wavelength of X-Ray used, L is the crystallite size. Rocking measurements gained from different symmetric and asymmetric planes are used to draw cosΘ versus 1/FWHM plot. Slope of this plot gives us crystallite size. In Figure 1 Plots of cosθ vs 1/β gained from Scherrer method can be seen.

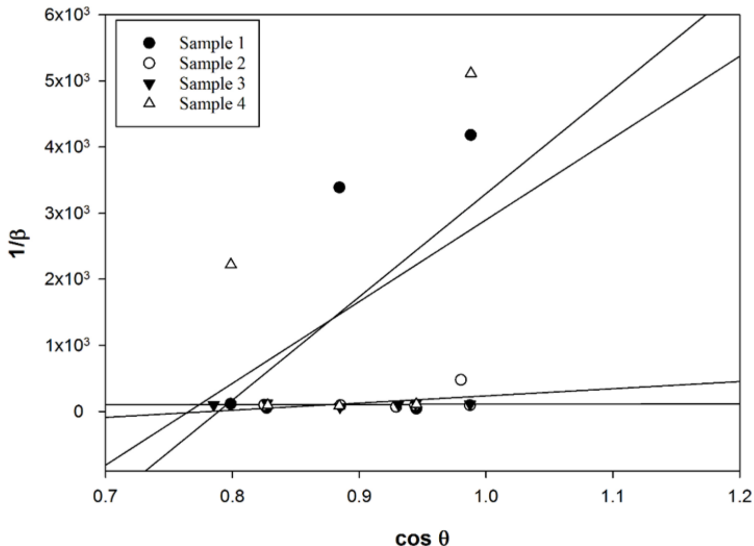

Figure 1. *Plots of cosθ vs 1/β gained from Scherrer method*

In Scherrer and modified Scherrer methods related with HR-XRD data and WH method are used in UDM, USDM and UDEDM models to calculate crystallite size, micro-structure strain and stress. During these calculations rocking curves and 2Θ measurements are used. It is noticed that these two measurement results are in agreement. Results are discussed in conclusion section.

HR-XRD graphic of aluminum nitrate buffer layers grown on silicon-on carbide substrate are shown in Figure 2. Top points of AlN buffer layers for (00.2), (00.4) and (00.6) diffraction planes can be seen in Figure 2. Peak points for all samples exhibit variations in peak widths. This situation is interested in mosaic crystally. Results are discussed in Table 2.

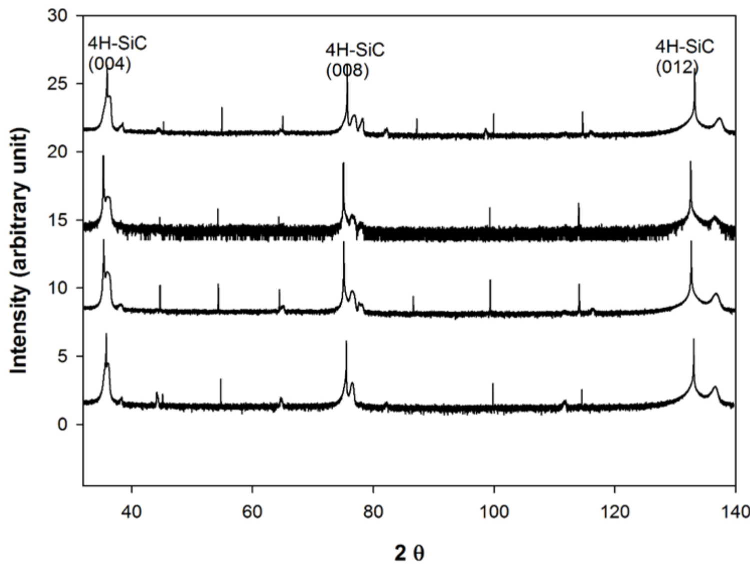

Figure 2. *High resolution Bragg reflection curves of samples 1, 2, 3 and 4 for (002), (004) and (006) planes*

Peak positions can be seen in Table 2 for different planes.

Table 2. *Peak positions of AlN buffer layers for samples 1, 2, 3 and 4 in degree.*

Sample No	1	2	3	4
(002)	36.45	36.06	36.22	36.54
(004)	77.29	77.47	76.83	76.57
(006)	136.82	136.52	137.01	137.11

In UDM method, equation (2) is derived from equation (1) by using some mathematical methods.

$$\beta_{hkl} = \beta T + \beta \varepsilon \tag{2}$$

$$\beta_{hkl} \cos(\theta_{hkl}) = \beta T + \beta \varepsilon \tag{3}$$

Because crystal defects are taken into account in this method, strain (ε) value can also be calculated by using equation (3). In Figure 3, βcosθ versus 4sinθ were plotted. Slope of linear fit calculates lattice strain value and crystallite size is determined by y-axis intercept of this fit. Because data are away from each other, most points are not fitted together.

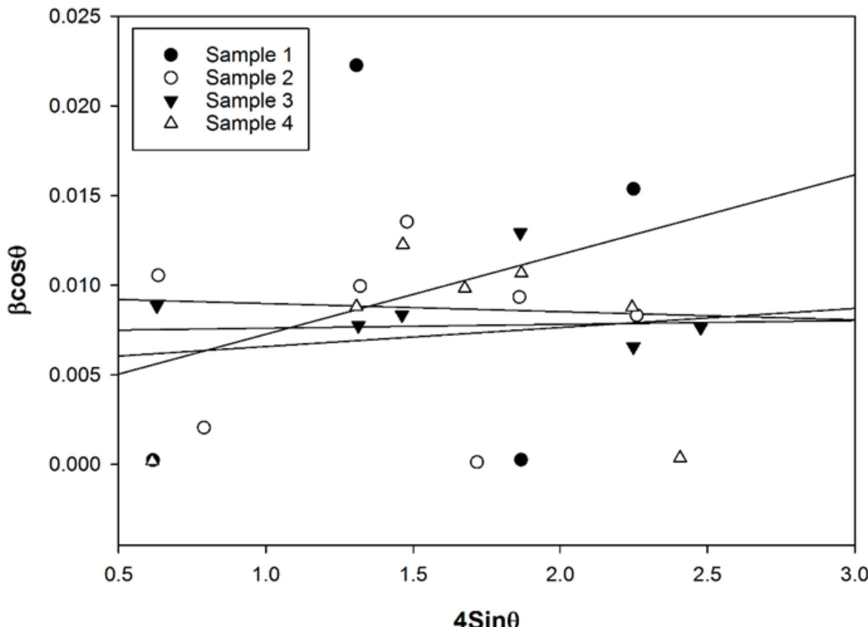

Figure 3. *βcosϴ vs 4sinϴ plot in modified WH method*

In USDM method $\sigma = \varepsilon E_{hkl}$ transformation gives modified Scherrer equation given in equation

$$\beta hkl = \frac{k\lambda}{D} + \frac{4\sigma sin\theta}{Ehkl} \tag{4}$$

If βcosϴ versus $4\sin\Theta / E_{hkl}$ plot is drawn given in Figure 4, crystallite size can be calculated from y-axis intercept of the fit. Slope of the fit gives us the strain. $\sigma = \varepsilon E_{hkl}$ equation can be used to calculate stress.

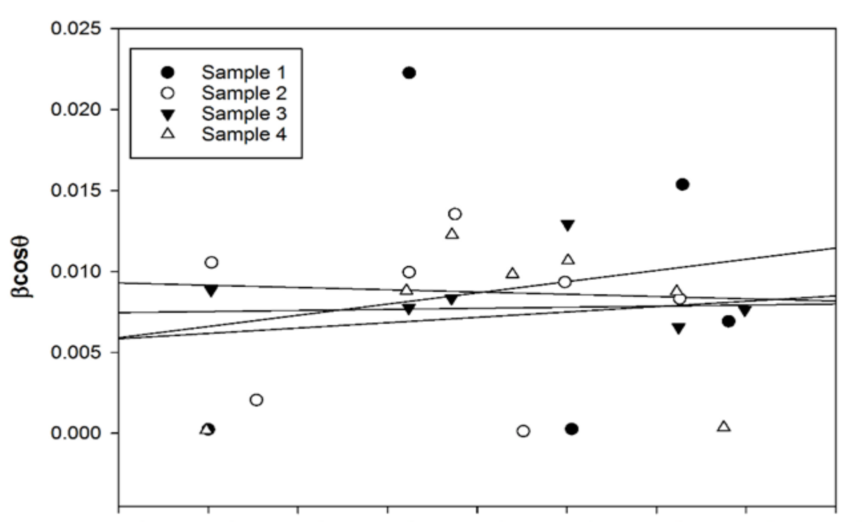

Figure 4. *βcosΘ vs (4sinΘ/E_{hkl}) plot for modified WH method*

If we compare Figure 3 and Figure 4, x axis data are different from each other. In UDEDM method if u=ε2$_{Ehkl}$/2 transformation is made, equation (5) is gained.

$$E_{hkl} = (h^2 + \frac{(h+2k)^2}{3} + \left(\frac{al^2}{c^2}\right) x(s_{11}(h^2 + \frac{(h+2k)^2}{3} + s_{33}\left(\frac{al^4}{c^4}\right)) \quad (5)$$

By using equation (5), if βcosΘ versus 4sinΘ(2/E_{hkl})0.5 plot is drawn, y-axis intercept of the fit gives crystallite size and slope of the fit gives UDED. u=ε2E_{hkl}/2 equation is used for calculating stress. In Figure 5 βcosθ vs (4sinθ(2/E_{hkl})$^{0.5}$) plot for modified WH method can be seen. Results are shown in Table 3 and it can be noticed that they are in good accordance with results of other models.

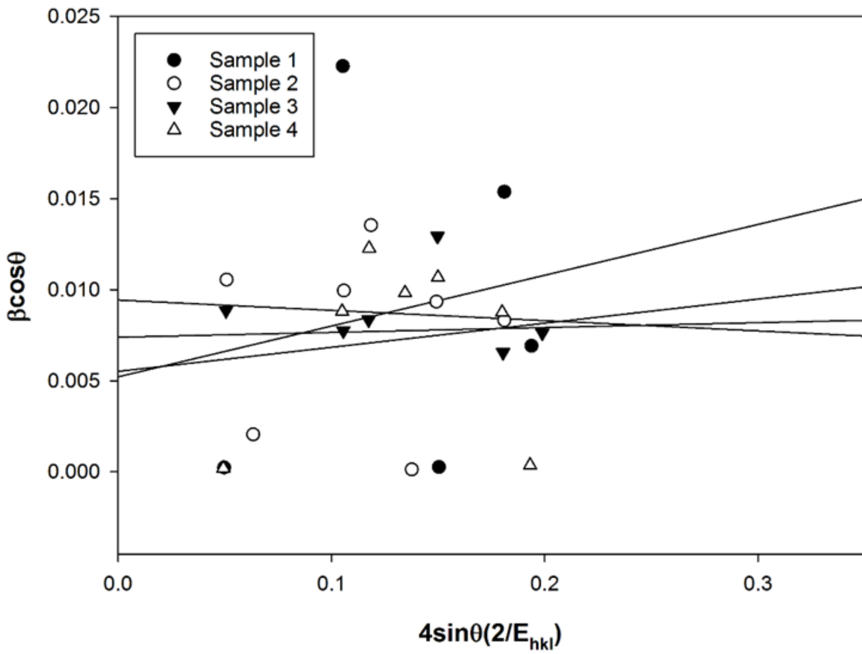

Figure 5. *βcosθ vs (4sinθ(2/E_{hkl})$^{0.5}$) plot for modified WH method*

Crystallite size determined by WH and Scherrer methods versus thickness for all samples is given in Table 4. For an optoelectronic device, crystallite of it is expected to be good. In ideal case, mono-crystal structure can be seen but many research showed that mentioned structures present mosaic form including high defects such as dislocation densities. Of course, for these research, using semi-experimental methods is effective. As can be seen in Table 4, crystallite size dependent on thickness increase until 140 nm and later it shows a decreasing behaviour. Crystallite size presents similar behaviour for Scherrer and WH methods.

In crystal structures, maintaining lattice match in c-orientation implies there is no strain. Strain in c-orientation causes cracks. Therefore, it must be examined. In Table 4, it can clearly be seen that strain gained with WH method is found at 10^{-3} level. It shows an increase from tension case to relaxation case. Around 140 nm thickness, near the region which relaxation increase rapidly versus tension, there is minimum critical thickness.

In samples, especially the ones including Al there is stress stemming from Al. In MOCVD technique, in the process of Al growth, forming Al is extremely difficult if proper temperature and pressure conditions are not maintained. Growth of Al is possible on SiC or sapphire but difference in band gaps may not permits to grow desired structures. For this reason, in Al based structures (especially AlN) permanent stress may occur.

Models are in accordance with each other. Table 4 presents a similar behaviour with thickness versus strain. Here relaxation after tension behaviour can be noticed for samples 1, 2 and 3. Also critical minimum around 140 nm can be seen here.

Table 3. *Mosaic defects of samples*

Sample	1	2	3	4
N_{edge} ($x10^{10}$ cm^{-2})	56.19	32.78	8.99	2.98
N_{screw}($x10^{8}$ cm^{-2})	19.64	6.31	1.41	2.46
L_{ort}(nm)	108.88	1952.62	1405.58	156.85
L_{par}(nm)	45.93	974.49	841.36	81.65
Tilt	0.019	0.011	0.015	0.016
Stress	$-1.72x10^{-3}$	$-2.26x10^{-3}$	$-2.5x10^{-3}$	$-2.63x10^{-3}$

Table 4. *Samples Scherrer, UDM, USDM, UDEDM part dimensions physical size strain stress results with techniques*

		Scerrer			W-H method							$Sin^2\psi$
ID	Thick.	D(nm)	UDM		USDM			UDEDM				
	nm		D (nm)	ε ($x10^{-3}$)	D (nm)	σ (Gpa)	ε ($x10^{-3}$)	D (nm)	u(k)/m^3/($x10^{-3}$)	σ (Gpa)	ε ($x10^{-3}$)	σ (Gpa)
1	100	12.37	9.16	-2.61	9.44	-0.76	-2.43	9.27	1.01	-0.80	-2.54	-0.79
2	130	10.72	10.72	-2.09	11.48	-0.53	-1.70	10.95	0.56	-0.59	-1.91	-0.73
3	140	15.37	15.37	-2.06	12.71	-0.54	-1.74	12.18	0.57	-0.59	-1.91	-0.78
4	150	10.48	10.48	2.45	10.59	0.61	1.97	10.06	0.78	0.70	2.23	0.49

In Table 4, collected energy density from lattice versus thickness can be seen in UDEDM. In order to maintain the energy needed for tension to relaxation, energy value in this plot presents a sharp decreasing later increasing behaviour. This behaviour in thickness versus energy density implies, stress and strain situations are in good accordance.

Figure 6 shows strain analysis measurements for (00.2) plane of four samples. These measurements are repeated for every Ψ in θ-2θ scans. Ψ measurement range for all samples is -4°/4° with 0.2° unit steps. Scanning is made in this range for (00.2) planes which maintain Bragg condition. It is noticed that there is shift in the peaks for all samples. This situation implies there is stress and strain in the structures. The difference between samples can be seen in tables.

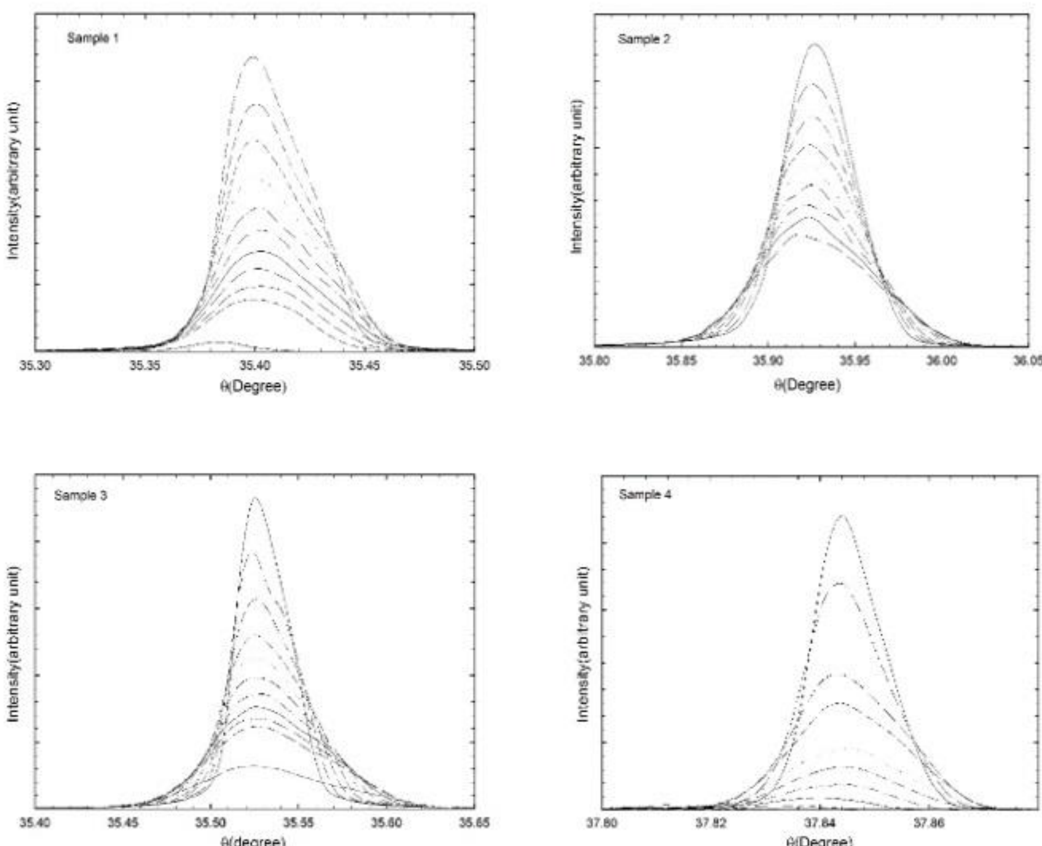

Figure 6. *Stress analysis of samples in (002) planes*

layer can form two situations: 1- $a_l<a_{os}$ (relaxation), 2- $a_l>a_{os}$ (tension). The reason for transmission from tension to relaxation around 140 nm due to critical thickness. If this value is surpassed, lattice coefficients of layers change.

-0.79 GPa (sample-1) (Yang et al., 2011), -0.73 GPa (sample-2), -0,78 GPa (sample-3) and 0,49 GPa (sample-4) (Pandey et al, 2021) values are gained from *sin2Ψ* method and they are in good accordance with WH models.

HR-XRD is a suitable method for investigation of mosaic defects. Because monocromatic Kα1 peak from Cu tube has high resolution (Williamson & William, 1953). Very few studies in literature takes attention with tilt and twist angle. For example, Lafford and co-workers investigated effect of alloy compounds and thickness on twist and tilt (Ayers, 1994). Wang and co-workers examined effect of grain volume on mosaical tilt and twist (Dai et al, 2018). For peak positions and broadening double axis x-ray pattern is used. In order to present quality of hexagonal structure, HR-XRD scans are used for symmetric and asymmetric planes. Surface morphology of samples is investigated with atomic force microscopy (AFM).

Hexagonal GaN and AlN based layers grown on Al_2O_3, SiC or Si presents lattice mismatch. As the result of this mismatch, it shows high dislocation density. There are 3 types of dislocations in such layers. As, edge, screw and mixed type dislocations.

$$D_{edge} = (\frac{\beta^2}{9b^2}) \quad (6)$$

Two methods are used for investigating tilt stemming from crystallity level and twist. In epitaxial layers it is possible to calculate Dedge and Dscrew (Ambacher, 1998; Speck & Rosner, 1999) with equations (6) and (7). Equation (7) is the same with equation (6). Full width at half maximum (FWHM) measured with HR-XRD states crystallity condition. Here b is the length of Burgers vector. (for AlN bscrew=0,4979 nm, bedge=0.3111 nm) (Chierchia et al., 2003).

Another method for edge and screw type dislocations is related with Burger's vector, plane tilt angle and lateral coherence length. All type of dislocations is dependent on, lateral coherence length of mosaic block, plane tilt and structure twist.

$$N_{(screw)} = (\frac{\alpha_{tilt}^2}{4.\ 35\ b\ screw^2}) \quad (7)$$

Screw type dislocation density can be calculated with equation (8).

Burger's vector is seen by azimuthal rotating of crystal along normal of c- surface. By measuring twist angle, edge type dislocation density can be calculated (Durukan et al., 2017).

$$N_{edge} = (\frac{\alpha\ \emptyset}{2.1\ b_{edge}\ L}) \quad (8)$$

In equation (8), αØ is FWHM of asymmetric planes, b is the length of lattice Burger's vector and L_l is the lateral coherence length (Bas et al., 2014).

HRXRD graphic of aluminum nitrate buffer layers grown on silicon carbide substrate is given in Figure 2. Peak positions of AlN buffer layers for (00.2), (00.4) and (00.6) symmetric planes can be explained in Figure 2. For four samples these peak positions show variations in peak broadening. This situation is depended on mosaic crystal structure.

Morphological properties of AlN/n-4H SiC structure is investigated by AFM. AFM scans are made in the range of 5μm x 5μm. Figure 7 shows (3D) AFM surface micrographs of AlN grown on 4H-SiC. AFM images show that layers have uniform and field like surface morphology. In addition to this, root mean square values (RMS) of samples are measured as 4.04, 3.72, 3.64 and 3.23 nm for samples 1, 2, 3 and 4 respectively. According to RMS values, 150 nm thick AlN layer grown with 50 sccm (NH3) flow ratio, has the smoothest surface morphology. It is obvious that if AlN layer is thicker, RMS value is lower for samples grown with the same NH3 flow ratio. This result implies structural quality of films increase with thicker buffer layers in accordance with XRD results. On the other hand, samples 3 which is grown with 1000 sccm NH3 flow ratio has rougher surface morphology than samples 4 which is grown with 50 sccm NH3 flow ratio. This result is in accordance with previous works done by different researchers (Çörekçi et al., 2012).

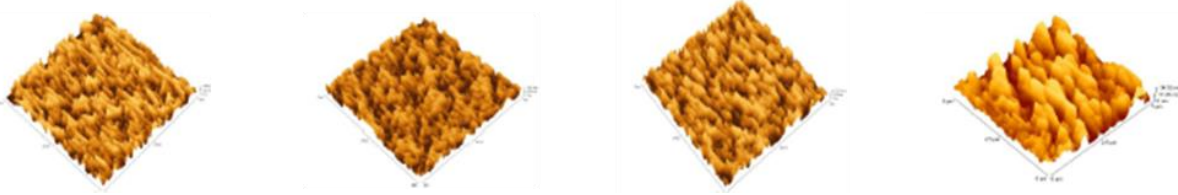

Figure 7. *(3D) AFM surface micrographs of samples4*

4. CONCLUSION

AlN buffer layers with different thickness are grown on SiC substrate by using Molecule beam epitaxy technique. Optical and structural properties of samples are investigated by using AFM and HR-XRD systems. Strain calculation is made with symmetric and asymmetric peaks of AlN from HR-XRD. Peak positions are determined versus Ψ. For all samples WH models are applied to calculate strain, stress, crystallite size and energy density. Results are presented in table 4. In this table it is seen that energy value sharply decrease later increase. This behaviour of energy density is in accordance with strain and stress behaviours. It is noticed that AlN buffer layers grown without tension and relaxation are more suitable for optoelectronic devices. For this reason, thickness optimization of AlN buffer layers is important.

ACKNOWLEDGEMENT

This work was supported by Presidency Strategy and Budget Directorate (Grants Number: 2016 K121220). Availability of Data and Materials All data used in this study are available from author.

AUTHOR CONTRIBUTIONS

O. Bayal, wrote the manuscript, D. Demir, made the measurements, A. K. Bilgili made the calculations, M. K. Ozturk, N. Kaya and S. Kalayci maintained device support.

CONFLICT OF INTEREST

The authors declare no conflict of interest.

REFERENCES

Akbas, S., Oztürk, M. K. (2023). Comparative study of neutronic, mechanical and thermodynamic properties of accident tolerant cladding materials: SiC, TiC and ZrC. *Materials Science and Engineering:* B, *290*, 116352. https://doi.org/10.2139/ssrn.4181421

Akpinar, O., Bilgili, A. K., Baskose, U. C., Ozturk, M. K., Ozcelik, S., & Ozbay, E. (2020). Swanepoel method for AlInN/AlN HEMTs. *Journal of Materials Science: Materials in Electronics*, *31*, 9969-9973. https://doi.org/10.31466/kfbd.954421

Ambacher, O. (1998). Growth and applications of group III-nitrides. *Journal of physics D: Applied Physics*, *31*(20), 2653. https://doi.org/10.1088/0022-3727/31/20/001

Ayers, J.E. (1994). The measurement of threading dislocation densities in semiconductor crystals by X-ray diffraction. *Journal of Crystal Growth*. *135*(1), 71-77. https://doi.org/10.1016/0022-0248(94)90727-7

Baş, Y., Demirel, P., Akın, N., Başköse, C., Özen, Yunus., Kınacı, Barış., & Özbay, E. (2014). Microstructural defect properties of InGaN/GaN blue light emitting diode structures. *Journal of Materials Science: Materials in Electronics*, *25*, 3924-3932.

Chierchia, R., Böttcher, T., Heinke, H., Einfeldt, S., Figge, S., & Hommel, D. (2003). Microstructure of heteroepitaxial GaN revealed by x-ray diffraction. *Journal of Applied physics*, *93*(11), 8918-8925. https://doi.org/10.1063/1.1571217

Çörekçi, S., Öztürk, M. K., Çakmak, M., Özçelik, S., & Özbay, E. (2012). The influence of thickness and ammonia flow rate on the properties of AlN layers. *Materials Science in Semiconductor Processing*, *15*(1), 32-36. https://doi.org/10.1016/j.mssp.2011.06.003

Durukan, İ. K., Öztürk, M. K., Özçelik, S., & Özbay, E. (2017). Analysis of the Mosaic Defects in Graded and Non Graded In x Ga 1-x N Solar Cell Structures. *Süleyman Demirel Üniversitesi Fen Bilimleri Enstitüsü Dergisi*, *21*(1), 235-240. https://doi.org/10.19113/sdufbed.58096

Lester, S. D., Ponce, F. A., Craford, M. G., & Steigerwald, D. A. (1995). High dislocation densities in high efficiency GaN-based light-emitting diodes. *Applied Physics Letters*, *66*(10), 1249-1251.

Lin, M. E., Sverdlov, B., Zhou, G. L., & Morkoc, H. (1993). A comparative study of GaN epilayers grown on sapphire and SiC substrates by plasma-assisted molecular-beam epitaxy. *Applied Physics Letters*, *62*(26), 3479-3481. https://doi.org/10.1063/1.109026

Mote, V.D., Y. Purushothani, & Dole B.N. (2012). Williamson-Hall analysis in estimation of lattice strain in nanometer-sized ZnO particles. *Journal of Theoretical and Applied Physics*, *6*(1). https://doi.org/10.1186/2251-7235-6-6

Nakamura, S. (1995). InGaN/AlGaN Blue-Light-Emitting Diodes. *Journal of Vacuum Science & Technology A*, *13*(3), 705-710. https://doi.org/10.1116/1.579811

Nakamura, S., Mukai, T., & Senoh, M. (1994). Candela-class high-brightness InGaN/AlGaN double-heterostructure blue-light-emitting diodes. *Applied Physics Letters*, *64*(13), 1687-1689. https://doi.org/10.1063/1.111832

Nakamura, S., Senoh, M., Iwasa, N., & Nagahama, S. I. N. S. I. (1995). High-brightness InGaN blue, green and yellow light-emitting diodes with quantum well structures. *Japanese Journal of Applied Physics*, *34*(7A), L797. https://doi.org/10.1143/JJAP.34.L797

Pandey, A., Shankar, D., Janesh, K., Nidhi, G., Garima, G., Raman, R., Davinder, K. (2021). Growth, structural and electrical properties of AlN/Si (111) for futuristic MEMS applications. *Materials Science in Semiconductor Processing*, *123*, 105567. https://doi.org/10.1016/j.mssp.2020.105567

Rong, X., Wang, X., Chen, G., Pan, J., Wang, P., Liu, H., & Shen, B. (2016). Residual stress in AlN films grown on sapphire substrates by molecular beam epitaxy. *Superlattices and Microstructures*, *93*, 27-31. https://doi.org/10.1016/j.spmi.2016.02.050

Sasaki, T., & Matsuoka, T. (1988). Substrate-polarity dependence of metal-organic vapor-phase epitaxy-grown GaN on SiC. *Journal of Applied Physics*, *64*(9), 4531-4535. https://doi.org/10.1063/1.341281

Speck, J. S., & Rosner, S. J. (1999). The role of threading dislocations in the physical properties of GaN and its alloys. *Physica B: Condensed Matter*, *273*, 24-32. https://doi.org/10.1016/S0921-4526(99)00399-3

Uehara, K., Yang, C. M., Furusho, T., Kim, S. K., Kameda, S., Nakase, H., & Tsubouchi, K. (2003). AlN epitaxial film on 6H-SiC (0001) using MOCVD for GHz-band saw devices. In IEEE Symposium on Ultrasonics. Vol. 1, pp. 905-908. IEEE. https://doi.org/10.1109/ULTSYM.2003.1293546

Williamson, G.K. & W.H. Hall. (1953). X-ray line broadening from filed aluminium and wolfram. *Acta Metallurgica*, *1*(1), 22-31. https://doi.org/10.1016/0001-6160(53)90006-6

Yang, S., Reina, M., Hideto, M., Kazumasa, H., & Hiroshi, H. (2011). Raman Scattering Spectroscopy of Residual Stresses in Epitaxial AlN Films. *Applied Physics Express*, 4(3), 031001. https://doi.org/10.1143/APEX.4.031001